J Inf Process Syst, Vol.12, No.4, pp.765~778, December 2016
http://dx.doi.org/10.3745/JIPS.03.0055

ISSN 1976-913X (Print)
ISSN 2092-805X (Electronic)

JOURNAL OF INFORMATION PROCESSING SYSTEMS JIPS

Blind Color Image Watermarking Based on DWT and LU Decomposition

Dongyan Wang*, Fanfan Yang*, and Heng Zhang*

Abstract

In watermarking schemes, the discrete wavelet transform (DWT) is broadly used because its frequency component separation is very useful. Moreover, LU decomposition has little influence on the visual quality of the watermark. Hence, in this paper, a novel blind watermark algorithm is presented based on LU transform and DWT for the copyright protection of digital images. In this algorithm, the color host image is first performed with DWT. Then, the horizontal and vertical diagonal high frequency components are extracted from the wavelet domain, and the sub-images are divided into 4×4 non-overlapping image blocks. Next, each sub-block is performed with LU decomposition. Finally, the color image watermark is transformed by Arnold permutation, and then it is inserted into the upper triangular matrix. The experimental results imply that this algorithm has good features of invisibility and it is robust against different attacks to a certain degree, such as contrast adjustment, JPEG compression, salt and pepper noise, cropping, and Gaussian noise.

Keywords

Digital Color Image Watermark, Discrete Wavelet Transformation (DWT), LU Decomposition, Normalized Correlation (NC), Structural Similarity (SSIM)

1. Introduction

With the speedy evolution of information technology and the increasing usage of the internet, digital products are being widely applied in every field of people's lives. Although these products bring convenience to people, they also bring more and more serious problems at the same time, such as information infringement and unauthorized tampering. As one of the important ways to avoid violations and illegal manipulations, image watermarking is getting more and more attention.

As there are not any universally accepted standard on digital watermarking technology currently, watermark researchers are working hard to create a unified digital watermark standard. However, the invisibility and robustness of digital watermarking are two features that are difficult to balance, so it is extremely hard to form a general and effective standard. Many experts and scholars have made important contributions to digital watermarking, and many novel algorithms have been proposed.

At present, digital watermarking methods mainly include two types [1]: spatial and frequency domains. A spatial domain-based digital watermarking scheme embeds watermark information via

Manuscript received July 9, 2015; accepted January 6, 2016.
Corresponding Author: Dongyan Wang (wdysdu@gmail.com)
* School of Mechanical, Electrical and Information Engineering, Shandong University, Weihai, China (wdysdu@gmail.com, {yangfanfanwh, sdwhzh}@163.com)

controlling the pixel values of the carrier image. The least significant bit (LSB) algorithm [2] is the most widely used technique in spatial domain watermarking. In this method, watermark information is directly embedded into one or multiple bit-planes of images. The LSB algorithm has the advantage of better imperceptibility and lower computational complexity. However, it has poor robustness, which makes it unable to resist image transmission, compression, and other common operations. In frequency domain based watermarking schemes, the watermark message is inserted into the frequency coefficients of the carrier image. The host image is first transformed into the frequency domain and then the watermark information is adopted to adjust the transformed coefficients. The most classical frequency domain-based watermark technique adopts the discrete cosine transform (DCT) [3], which is robust against image filtering, compression, and other processing operations. It is also compatible with JPEG compression. As for the DCT domain digital watermarking algorithm, it mainly embeds the watermarking information into low frequencies of the host image. The reason is that high frequencies are vulnerable to a variety of signal processing attacks.

In recent years, watermarking algorithms based on the discrete wavelet transform (DWT) [4,5], discrete Fourier transform (DFT) [6], integer wavelet transform (IWT) [7], singular value decomposition (SVD) [8], and other complicated transforms [9,10] have been introduced one after another. In the aforementioned methods, the common feature is that watermark insertion is completed by the modulation of low-frequency components. It is well-known that IWT has no rounding errors when it is applied to map integer to integer. The watermarked image obtained by the watermarking method based on IWT has good imperceptibility. A blind watermarking algorithm based on state coding was proposed by Su et al. [11], in which a color watermark image is inserted into a color host image. IWT and the state coding rules were performed while embedding the watermark. In watermark extraction, the watermark was obtained from the watermarked image by using the state coding without the help of the original watermark and carrier image. However, this method is not yet fully effective under JPEG compression. As is well known, grayscale images are often adopted as host images in most current SVD-based watermarking schemes, and color images are rarely used in their watermarks [12,13]. Furthermore, in general, watermark extraction is completed by a non-blind method. For example, in [12], three matrices ($\boldsymbol{S}, \boldsymbol{U}_{\mathrm{w}}, \boldsymbol{V}_{\mathrm{w}}$) are stored in advance in the watermark embedding process, and they are adopted once again in the receiver to extract the watermark. In recent watermarking schemes, DWT has been significantly used as well. This is a popular method for the analysis of multi-resolution in time and frequency. Lu et al. [14] introduced a robust watermarking method that combined DWT and sub-sampling techniques. A random sequence in Gaussian distribution was regarded as a watermark and inserted into the DWT domain. In the watermark extraction step, the correlation between the watermarked frames and watermark was calculated to detect the watermark. Inserting two different types of watermarks into a digital image increased the security of data hiding mechanism. Given this, Bekkouch and Faraoun [15] proposed a robust and reversible watermarking algorithm by using a combination of DWT, DCT, and SVD decomposition. In their method, two types of watermarks with different functions are embedded into the singular values in the DWT domain. The first kind of watermark is employed for image authentication, while the second kind of watermark is adopted to prove confidentiality. Jane and Elbasi [16] proposed a non-blind watermarking method using the combination of SVD and DWT by LU transform, in which a binary image was embedded in the low-band in the wavelet domain by using LU decomposition. Their experimental results proved that this method is reliable and it can resist many attacks without degrading the quality of the input image.

However, the robustness provided in this method is not good enough, and the similarity ratio of the extracted watermark is lower than 0.9 under various attacks.

The truth is that the digital color image is more widely used than the grayscale image. Motivated by this fact, blind color watermarking method is a demand for copyright protection of color images. The biggest challenge is how to make a trade-off between high visual quality and robustness against commonly used attacks. The key problem for image copyright protection is to enhance robustness and security. The safety of the watermarking scheme will be further reinforced by suitable encryption method.

In this paper, blind color image watermarking using DWT and LU decomposition [17] is presented. The watermark information is inserted into the $\boldsymbol{U}$ matrix in the DWT domain. In order to strengthen security, the Arnold transform has been adopted. The main contribution of our work is to present a blind image watermarking scheme that has stronger invisibility and better robustness under different attacks.

The rest of this paper is organized as follows: in Section 2, related works about the Arnold transform, DWT, and LU decomposition are introduced. Section 3 describes the proposed watermarking scheme using DWT and LU decomposition. The experimental results and an in-depth discussion on the proposed method are presented in Section 4, and the conclusions are given in Section 5.

2. Related Works

2.1 Arnold Transform

The Arnold transform is broadly used as an encryption method [18]. The Arnold transform can be given as:

$$\begin{bmatrix} x' \\ y' \end{bmatrix} = \begin{bmatrix} 1 & 1 \\ 1 & 2 \end{bmatrix} \begin{bmatrix} x \\ y \end{bmatrix} \bmod N, \tag{1}$$

where (x, y) and (x', y') denote the pixel values in the original image and the transformed one, respectively. N is the size of the image, and the Arnold transform can be used to hide information. In addition, in order to enhance the safety and confidentiality of the method, the Arnold transform takes the transform times as the encryption key E. In the algorithm given in this paper, Arnold scrambling is respectively executed for the R, G, and B components of the embedded watermark. In watermark extraction, the encryption key E is used for decryption to reconstruct the original watermark.

2.2 Discrete Wavelet Transform

The wavelet transform is playing a more and more important role in image processing. The two-dimensional (2-D) DWT is widely used in image watermarking. By using 2-D DWT, optimal embedding positions are selected for watermark insertion, and the robustness and imperceptibility of the watermark could be better balanced. Fig. 1 shows the schematic diagram of a color image decomposed by a one-level DWT. For example, we applied 2-D DWT to the G channel and obtained

the decomposition result. The same operation is applied to the R, G, and B components. The carrier image is then split into four sub-bands, which are one low-frequency component (approximation) and three high-frequency components (details) located in the horizontal, vertical, and diagonal directions, respectively. These four sub-band images are referred to as: LL, HL, LH, and HH, in which LL is the low-frequency sub-band and HL, LH, and HH are the high-frequency sub-bands.

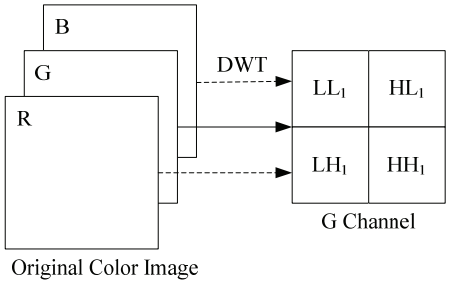

Fig. 1. One-level DWT transform of original color host image.

2.3 LU Decomposition

As for the theory of matrices in matrix analysis, the LU transform given by Turing [17] in 1948 can be used as the basic modified way of Gaussian elimination. The LU transform is often adopted in solving square systems of linear equations. In other words, the LU transform is a necessary process when calculating the determinant of a matrix or inverting a matrix.

The LU transform inverts a matrix $\boldsymbol{A}$ as the product of an upper triangular matrix $\boldsymbol{U}$ and a lower triangular matrix $\boldsymbol{L}$. Sometimes, a permutation matrix can also be obtained. For example, for a 4×4 matrix $\boldsymbol{A}$, its LU decomposition can be presented as:

$$\begin{aligned}\boldsymbol{A} &= [\boldsymbol{a}_1,\boldsymbol{a}_2,\boldsymbol{a}_3,\boldsymbol{a}_4] = \begin{bmatrix} a_{11} & a_{12} & a_{13} & a_{14} \\ a_{21} & a_{22} & a_{23} & a_{24} \\ a_{31} & a_{32} & a_{33} & a_{34} \\ a_{41} & a_{42} & a_{43} & a_{44} \end{bmatrix} \\ &= \boldsymbol{LU} = [\boldsymbol{l}_1,\boldsymbol{l}_2,\boldsymbol{l}_3,\boldsymbol{l}_4][\boldsymbol{u}_1,\boldsymbol{u}_2,\boldsymbol{u}_3,\boldsymbol{u}_4] = \begin{bmatrix} 1 & 0 & 0 & 0 \\ l_{21} & 1 & 0 & 0 \\ l_{31} & l_{32} & 1 & 0 \\ l_{41} & l_{42} & l_{43} & 1 \end{bmatrix} \begin{bmatrix} u_{11} & u_{12} & u_{13} & u_{14} \\ 0 & u_{22} & u_{23} & u_{24} \\ 0 & 0 & u_{33} & u_{34} \\ 0 & 0 & 0 & u_{44} \end{bmatrix}. \end{aligned} \tag{2}$$

Then we can obtain:

$$\boldsymbol{A} = \begin{bmatrix} u_{11} & u_{12} & u_{13} & u_{14} \\ l_{21}u_{11} & l_{21}u_{12}+u_{22} & l_{21}u_{13}+u_{23} & l_{21}u_{14}+u_{24} \\ l_{31}u_{11} & l_{31}u_{12}+l_{32}u_{22} & l_{31}u_{13}+l_{32}u_{23}+u_{33} & l_{31}u_{14}+l_{32}u_{24}+u_{34} \\ l_{41}u_{11} & l_{41}u_{12}+l_{42}u_{22} & l_{41}u_{13}+l_{42}u_{23}+l_{43}u_{33} & l_{41}u_{14}+l_{42}u_{24}+l_{43}u_{34}+u_{44} \end{bmatrix}. \tag{3}$$

However, LU decomposition does not exist in all cases. Theorem 1 gives the conditions when the decomposition can be conducted.

Theorem 1. For $k=1:n-1$, if the determinant $\det(A(1:k,1:k))\neq 0$, A can be carried out for LU decomposition. If $\boldsymbol{A}$ is a nonsingular matrix and it is able to be decomposed by LU decomposition, there is only one LU decomposition and its $\det(\boldsymbol{A})=u_{11}u_{22}\cdots u_{nn}$.

3. Proposed Watermarking Scheme

DWT is a beneficial technique for multi-resolution analysis, and LU decomposition is a simple and fast method for conducting Gaussian elimination. Given these, a new blind watermark algorithm based on LU decomposition and DWT has been introduced for the copyright protection of color images. The main process is described in detail below.

3.1 Watermark Insertion

We selected the color host image I that was $N\times N$ in size and the color watermark image W that was $m\times m$ in size. The basic processes of watermark insertion are shown in Fig. 2. The embedding scheme is given below.

Step 1. The host image is disintegrated by a one-level DWT using a Haar filter, and then LL_1, HL_1, LH_1, and HH_1 sub-bands that are $(N/2)\times(N/2)$ in size are obtained.

Step 2. The high-frequency parts in horizontal and vertical diagonal positions, HL_1 and LH_1, are adopted as the embedding positions, and then these two sub-bands are divided into 4×4 non-overlapping blocks in the wavelet domain. There are $n=(N/2/4)\times(N/2/4)\times 2=N^2/32$ blocks in total, which are written as $\{\boldsymbol{b}_1,\boldsymbol{b}_2,\cdots,\boldsymbol{b}_i,\cdots,\boldsymbol{b}_n\}$.

Step 3. The LU decomposition is applied to each block of HL_1 and LH_1 sub-bands obtained in Step 1 by using Eq. (2) and, hence, $[\boldsymbol{L}_i,\boldsymbol{U}_i]=\mathrm{LU}(\boldsymbol{b}_i)$ is obtained. The $\mathrm{LU}(\cdot)$ refers to the operation of LU decomposition. The nonzero value $u_i(1,4)$ of $\boldsymbol{U}_i$ matrix is selected as the embedding position.

Step 4. The Arnold transform is applied to the color image watermark and the encryption key E is set. The watermark is converted into a sequence. Each element of this sequence is transformed into a bit stream of 8-bit binary numbers.

Step 5. The watermark information is embedded by using the quantization method in Eqs. (4) and (5). Δ is the quantization step, and k determines the intensity of watermark embedding. Then, $\boldsymbol{U}_i'$ and the watermarked block $\boldsymbol{b}_i'=\boldsymbol{L}\boldsymbol{U}_i'$ are obtained.

$$\begin{cases} k = \text{floor}[\text{ceil}(u_i(1,4)/\Delta)/2], \\ c_1 = 2k\Delta + 1.5\Delta, \\ c_2 = 2k\Delta - 0.5\Delta. \end{cases} \tag{4}$$

$$\begin{aligned} &\text{if } |u_i(1,4) - c_2| < |u_i(1,4) - c_1| \\ &\quad u_i'(1,4) = c_1; \\ &\text{else} \\ &\quad u_i'(1,4) = c_2; \\ &\text{end} \end{aligned} \tag{5}$$

Step 6. The inverse DWT (IDWT) is carried out, and then the watermarked image is obtained.

After the above steps, the untampered watermarked image is obtained. In order to evaluate its robustness, different attacks are usually added to the watermarked image. Once all of these procedures have been carried out, the watermark embedding is finished.

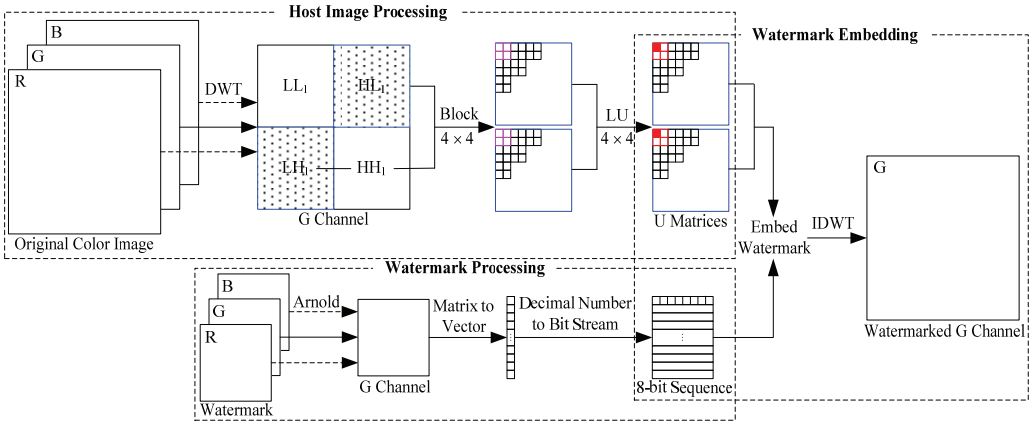

Fig. 2. Basic processes of watermark embedding.

3.2 Watermark Extraction

We obtained the watermarked version after the watermark insertion processes. At the receiving end, the color watermark can be extracted without the original watermark, so the proposed method is totally blind. The basic processes of watermark extraction are shown in Fig. 3. The watermark extraction steps are given in detail below.

Step 1. DWT with a Haar filter is applied to the watermarked image. Then LL_1, HL_1, LH_1, and HH_1 sub-bands are obtained.

Step 2. The high-frequency components in the horizontal and vertical diagonal positions, HL_1 and LH_1, which are the embedding positions, are used, and then these two sub-bands are divided into 4×4 non-overlapping blocks in the wavelet domain.

Step 3. The LU decomposition is applied to each block of the HL_1 and LH_1 sub-bands obtained in Step 1 by using Eq. (2) and the $\boldsymbol{U}$ matrices are obtained. According to the embedding positions, we were able to obtain the watermark information w_i of the R, G, and B components from the R, G, and B watermarked components based on Eq. (6), respectively. We also obtained the bit stream w_bit_i of the watermark based on Eq. (7).

$$w_i = \mathrm{mod}[\mathrm{ceil}(u_i^{\mathrm{w}}(1,4)/\Delta),2]\,. \tag{6}$$

$$\begin{aligned} &\text{if}\quad w_i == 1 \\ &\quad w\_bit_i = 1; \\ &\text{else} \\ &\quad w\_bit_i = 0; \\ &\text{end} \end{aligned} \tag{7}$$

Step 4. The bit stream obtained through binary decoding is disposed, and the scrambling watermark is obtained.

Step 5. According to the encryption key *E*, the color image watermark is reconstructed by using the inverse Arnold transform, and the extracted watermark is finally obtained.

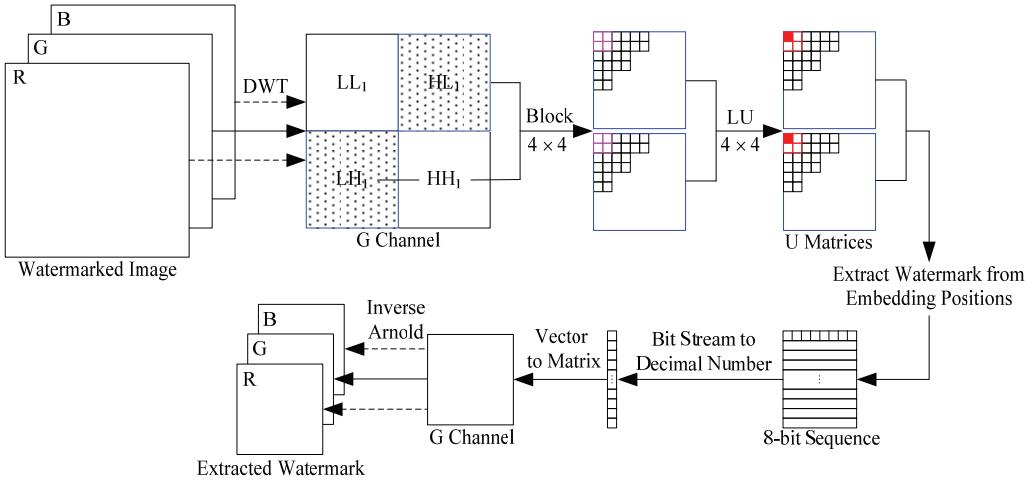

Fig. 3. Basic processes of watermark extraction.

4. Experimental Results and Discussion

Six typical 24-bit 512×512 color images were adopted as the initial carrier images, which are presented in Fig. 4(a)–(f). These images are from the CVG-UGR (Computer Vision Group-University of Granada) image database. Two 32×32 color images were used as the color watermark images, as shown in Fig. 5(a) and (b), which are the Shandong University (Weihai) logo and its letter image,

respectively. The one-level DWT using Haar filter was adopted in the watermark embedding and extracting processes. In this section, some simulation results are illustrated to prove the availability of the introduced method. Five types of attacks were used to test the robustness of the proposed scheme, which are contrast adjustment, salt and pepper noise, cropping, Gaussian noise, and JPEG compression.

After watermark embedding, the quality of the host image is reduced. In this paper, the peak signal-to-noise ratio (PSNR) was adopted to estimate the difference between the watermarked version and the original one. Another index is structural similarity (SSIM) [19]. Moreover, in order to test the quality of the extracted watermark, normalized correlations (NCs) were used to assess the similarity between the original watermark W and the extracted one W', which is defined as:

$$\mathrm{NC}=\frac{\sum_{j=1}^{3}\sum_{x=1}^{m}\sum_{y=1}^{m}[W(x,y,j)\times W'(x,y,j)]}{\sqrt{\sum_{j=1}^{3}\sum_{x=1}^{m}\sum_{y=1}^{m}[W(x,y,j)]^2}\sqrt{\sum_{j=1}^{3}\sum_{x=1}^{m}\sum_{y=1}^{m}[W'(x,y,j)]^2}}, \tag{8}$$

where $W(x,y,j)$ and $W'(x,y,j)$ represent the values in location (x,y), which are located in j components of the original watermark and its extracted version that is $m\times m$ in size.

The watermark was embedded into carrier images with different quantization steps, and then different SSIM and NC values were obtained. To address the balance between the robustness and invisibility of the watermark, the quantification step Δ is set to 30.

(a) (b) (c)

(d) (e) (f)

Fig. 4. Original host color images: (a) Lena, (b) Baboon, (c) Peppers, (d) Airplane, (e) Sailboat, and (f) House.

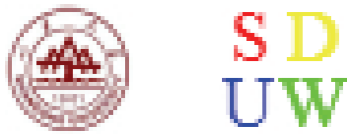

(a) (b)

Fig. 5. Original color image watermarks: (a) Shandong University (Weihai) logo and (b) letter image.

Table 1. Watermarked color images and their corresponding extracted watermarks without attacks

Color host images	Watermark in Fig. 2(a)		Watermark in Fig. 2(b)	
	Watermarked images (PSNR/SSIM)	Extracted watermarks (NC)	Watermarked images (PSNR/SSIM)	Extracted watermarks (NC)
	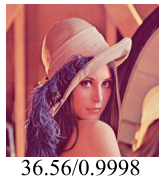 36.56/0.9998	 1	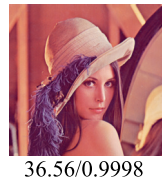 36.56/0.9998	 1
	 35.78/0.9999	 1	 35.83/0.9999	 1
	 36.10/0.9999	 1	 36.02/0.9999	 1
	 36.08/0.9999	 1	 36.09/0.9999	 1
	 36.14/0.9999	 1	 36.12/0.9999	 1
	 36.31/0.9999	 1	 36.31/0.9999	 1

4.1 Invisibility Test

Table 1 shows the watermarked images and the values of PSNR. It can be learned that the PSNR values are greater than 30 dB, which is a distinguishable value for the human eye. It demonstrates that the introduced scheme can obtain good watermark invisibility. The extracted watermarks from the corresponding watermarked images are shown in the third and fifth columns of Table 1, respectively. As can be seen, the watermarks can be easily obtained from the watermarked images via the proposed scheme.

Table 2. NC values and comparison between the proposed scheme and Su et al. [11] under different attacks

Attack	Parameter	Su et al. [11]	Proposed method
Contrast adjustment	Default	0.9136	0.9912
JPEG compression	90	0.9139	0.9580
	95	0.9176	0.9714
Salt and pepper noise	0.1	0.9233	0.9854
	0.2	0.9163	0.9731
	0.3	0.9153	0.9602
Cropping	1/16	0.9259	0.9663
	1/8	0.9287	0.9325
	1/4	0.9350	0.8627
	1/2	0.9397	0.7041
Gaussian noise	0.1	0.9295	0.9897
	0.2	0.9392	0.9570

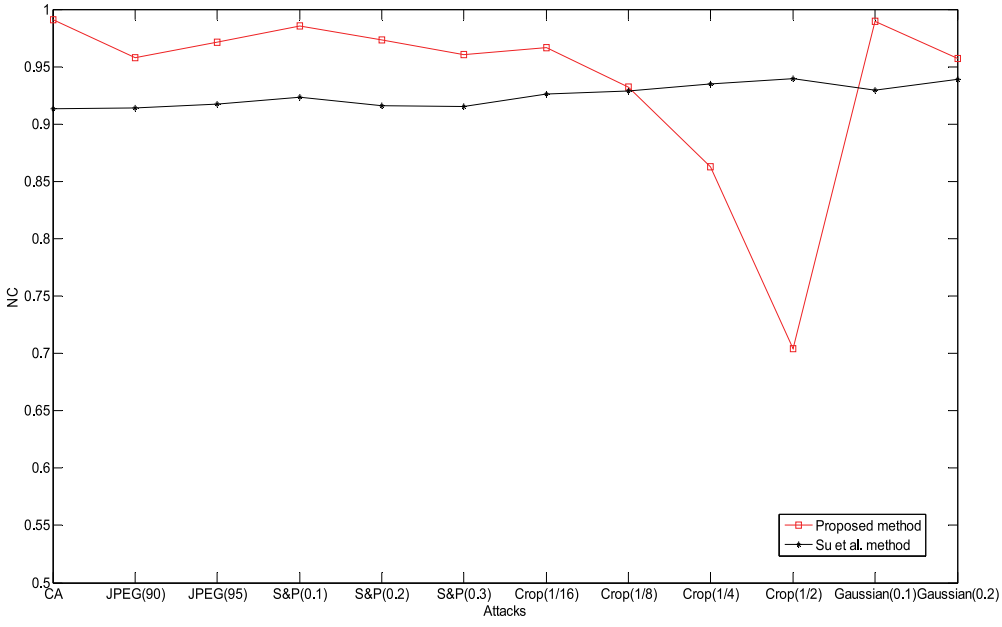

Fig. 6. NC value curves of extracted watermarks obtained by different methods under different attacks.

Fig. 7. Watermarked images after adding different kinds of attacks: (a) contrast adjustment (default), (b) JPEG compression (QF=90), (c) JPEG compression (QF=95), (d) salt and pepper noise (0.01), (e) salt and pepper noise (0.02), (f) salt and pepper noise (0.03), (g) Gaussian noise (0.1), (h) Gaussian noise (0.2), (i) cropping (1/16), (j) cropping (1/8), (k) cropping (1/4), and (l) cropping (1/2).

4.2 Robustness Test

In order to evaluate the robustness of our watermarking method, the following different attacks were added: contrast adjustment (MATLAB default setting), JPEG compression with a quality factor (QF) of 90 and 95, salt and pepper noise (density was 0.1, 0.2, and 0.3), cropping (cropping area was accounted for 1/16, 1/8, 1/4, and 1/2), and Gaussian noise (the mean was 0.1 and 0.2). We also compared the NC values of Su et al. [11] and our proposed scheme. Table 2 and Fig. 6 display the experimental results of the above methods under different attacks. In addition to cropping (1/4 and 1/2), the NC values of the proposed method were larger than the scheme given in [11]. In our proposed method, the positions of the embedded watermark were located in the whole image, which resulted in poor reconstructions when the watermarked image was cropped too much, such as by 1/4 and 1/2. In regards to the other four attacks, our method was more robust than the algorithm in [11]. Fig. 7 shows the watermarked images after different attacks were added, and Fig. 8 illustrates the extracted watermarks after corresponding attacks. In short, our proposed method achieved good performances both subjectively and objectively.

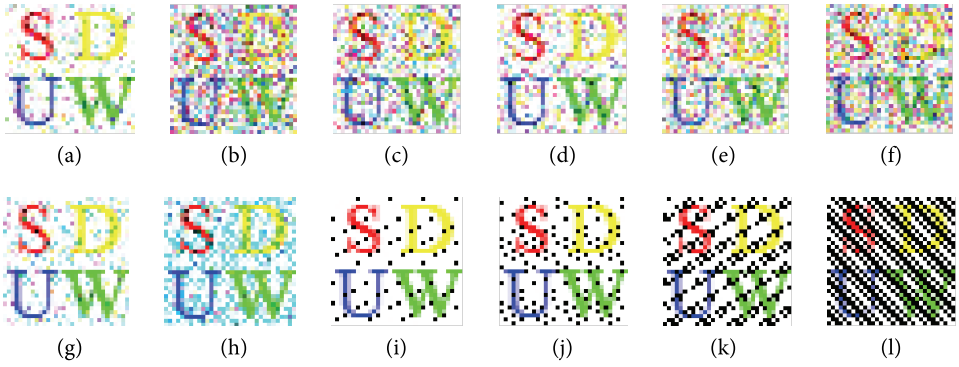

Fig. 8. Extracted watermarks after adding different kinds of attacks: (a) contrast adjustment (default), (b) JPEG compression (QF=90), (c) JPEG compression (QF=95), (d) salt and pepper noise (0.01), (e) salt and pepper noise (0.02), (f) salt and pepper noise (0.03), (g) Gaussian noise (0.1), (h) Gaussian noise (0.2), (i) cropping (1/16), (j) cropping (1/8), (k) cropping (1/4), and (l) cropping (1/2).

5. Conclusions

In this paper, a blind digital watermarking algorithm based on a DWT and LU transform has been proposed for the copyright protection of color images. Experimental results indicated that this scheme provides good performance in regards to robustness and invisibility. This scheme is also more robust against some common image processing attacks, such as contrast adjustment, salt and pepper noise, cropping, Gaussian noise, and JPEG compression. In addition, the Arnold transform was used on the watermark so that the security of the watermark would be improved. Our method is very easy to operate, and it can reduce the amount of memory used in digital products. The above features are highly significant for technologies such as mobile phones and other embedded systems that lack enough resources.

Acknowledgement

The 7th Undergraduate Research Apprentice Program (URAP) and the 11th Student Research Training Program (SRTP) at Shandong University, Weihai, China, and the Natural Science Foundation of Shandong Province, China (No. ZR2015PF004) supported this work. Dongyan Wang thanks Associate Professor Chengyou Wang and Dr. Xiao Zhou, who work at the Image Processing and Computer Vision (IPCV) research group, for giving her the opportunity to do some research as a research assistant. The authors also thank Yunpeng Zhang and Liping Wang for their generous assistance in revising this paper.

References

[1] R. G. van Schyndel, A. Z. Tirkel, and C. F. Osborne, "A digital watermark," in *Proceedings of the IEEE International Conference on Image Processing*, Austin, TX, USA, 1994, pp. 86-90.

[2] Z. Y. An and H. Y. Liu, "Research on digital watermark technology based on LSB algorithm," in *Proceedings of the 4th International Conference on Computational and Information Sciences*, Chongqing, China, 2012, pp. 207-210.

[3] J. Y. Zheng, D. H. Ling, J. Z. Liang, and M. Jin, "A DCT-based digital watermarking algorithm for image," in *Proceedings of the International Conference on Industrial Control and Electronics Engineering*, Xi'an, China, 2012, pp. 1217-1220.

[4] C. C. Lai and C. C. Tsai, "Digital image watermarking using discrete wavelet transform and singular value decomposition," *IEEE Transactions on Instrumentation and Measurement*, vol. 59, no. 11, pp. 3060-3063, 2010.

[5] K. Ramanjaneyulu and K. Rajarajeswari, "Wavelet-based oblivious image watermarking scheme using genetic algorithm," *IET Image Processing*, vol. 6, no. 4, pp. 364-373, 2012.

[6] M. Urvoy, D. Goudia, and F. Autrusseau, "Perceptual DFT watermarking with improved detection and robustness to geometrical distortions," *IEEE Transactions on Information Forensics and Security*, vol. 9, no. 7, pp. 1108-1119, 2014.

[7] C. Y. Yang, "High-payload digital watermarking using radius-weighted mean based on IWT domain," in *Proceedings of the 9th International Conference on Intelligent Information Hiding and Multimedia Signal Processing*, Beijing, China, 2013, pp. 68-71.

[8] R. S. Run, S. J. Horng, J. L. Lai, T. W. Kao, and R. J. Chen, "An improved SVD-based watermarking technique for copyright protection," *Expert Systems with Applications*, vol. 39, no. 1, pp. 673-689, 2012.

[9] O. Jane, E. Elbasi, and H. G. Ilk, "Hybrid non-blind watermarking based on DWT and SVD," *Journal of Applied Research and Technology*, vol. 12, no. 4, pp. 750-761, 2014.

[10] B. Y. Lei, I. Y. Soon, and Z. Li, "Blind and robust audio watermarking scheme based on SVD-DCT," *Signal Processing*, vol. 91, no. 8, pp. 1973-1984, 2011.

[11] Q. T. Su, Y. G. Niu, X. X. Liu, and Y. Zhu, "A blind dual color images watermarking based on IWT and state coding," *Optics Communications*, vol. 285, no. 7, pp. 1717-1724, 2012.

[12] R. A. Ghazy, N. A. El-Fishawy, M. M. Hadhoud, M. I. Dessouky, and F. E. S. Abd El-Samie, "Performance evaluation of block based SVD image watermarking," *Progress In Electromagnetics Research B*, vol. 8, pp. 147-159, 2008.

[13] I. A. Ansari, M. Pant, and F. Neri, "Analysis of gray scale watermark in RGB host using SVD and PSO," in *Proceedings of the IEEE Symposium on Computational Intelligence for Multimedia, Signal and Vision Processing*, Orlando, FL, USA, 2014, pp. 1-7.

[14] W. Lu, W. Sun, and H. T. Lu, "Novel robust image watermarking based on subsampling and DWT," *Multimedia Tools and Applications*, vol. 60, no. 1, pp. 31-46, 2012.

[15] S. Bekkouch and K. M. Faraoun, "Robust and reversible image watermarking scheme using combined DCT-DWT-SVD transforms," *Journal of Information Processing Systems*, vol. 11, no. 3, pp. 406-420, 2015.

[16] O. Jane and E. Elbasi, "A new approach of nonblind watermarking methods based on DWT and SVD via LU decomposition," *Turkish Journal of Electrical Engineering and Computer Sciences*, vol. 22, no. 5, pp. 1354-1366, 2014.

[17] A. M. Turing, "Rounding-off errors in matrix processes," *The Quarterly Journal of Mechanics and Applied Mathematics*, vol. 1, no. 1, pp. 287-308, 1948.

[18] L. Lu, X. D. Sun, and L. T. Cai, "A robust image watermarking based on DCT by Arnold transform and spread spectrum," in *Proceedings of the 3rd International Conference on Advanced Computer Theory and Engineering*, Chengdu, China, 2010, pp. 198-201.

[19] Z. Wang, A. C. Bovik, H. R. Sheikh, and E. P. Simoncelli, "Image quality assessment: from error visibility to structural similarity," *IEEE Transactions on Image Processing*, vol. 13, no. 4, pp. 600-612, 2004.

Dongyan Wang http://orcid.org/0000-0003-2930-2689

She was born in Shandong province, China, in 1996. She was admitted into Shandong University, Weihai, China, in 2014. Her major is computer science and technology. Her current research interests include digital image processing and computer vision.

Fanfan Yang http://orcid.org/0000-0002-6997-2735

She was born in Shandong province, China, in 1989. She received her B.E. degree in communication engineering from Shandong University, Weihai, China, in 2013 and her M.E. degree in communication and information system from Shandong University, China, in 2016. She is currently with the Goertek Inc., Weifang, China. Her current research interests include acoustic and audio signal processing, blind image forensics, and computer vision.

Heng Zhang http://orcid.org/0000-0003-1864-5432

He was born in Shandong province, China, in 1991. He received his B.E. degree in communication engineering from Shandong University of Technology, China, in 2015. He is currently pursuing his M.E. degree in electronics and communication engineering at Shandong University, China. His current research interests include watermarking-based image authentication and computer vision.